

# Embedment properties of thermally modified spruce timber with dowel-type fasteners

Joran van Blokland<sup>a,\*</sup>, Sara Florisson<sup>b</sup>, Michael Schweigler<sup>c</sup>, Torbjörn Ekevid<sup>d</sup>, Thomas K. Bader<sup>c</sup>, Stergios Adamopoulos<sup>a</sup>

<sup>a</sup> Department of Forest Biomaterials and Technology, Swedish University of Agricultural Sciences, Uppsala, Sweden

<sup>b</sup> Division of Wood Science and Engineering, Luleå Technical University, Skellefteå, Sweden

<sup>c</sup> Department of Building Technology, Linnaeus University, Växjö, Sweden

<sup>d</sup> Volvo Construction Equipment, Gothenburg, Sweden

## ARTICLE INFO

### Keywords:

ASTM D 5764-97a  
Embedment stiffness  
Embedment strength  
EN 383  
Foundation modulus  
Full-hole test  
Half-hole test  
Norway spruce  
ThermoWood®

## ABSTRACT

This study investigates the effect of thermal modification, ThermoWood Thermo-D treatment versus no treatment, on the embedment properties of Norway spruce timber (*Picea abies* [L.] Karst.) with dowel-type fasteners. The test specimens were reinforced to prevent splitting of the wood. The influence of density, load direction, test specimen configuration (full hole versus half hole), moisture content, gauge points and calculation method were also evaluated. Thermal modification primarily affected the embedment strength parallel to the grain, which was ~ 25% higher after thermal modification, mainly due to the change in physical properties because of the treatment, i.e. the lower equilibrium moisture content. The influence of the investigated parameters on embedment properties of thermally modified spruce followed similar trends as for unmodified spruce. It was for example seen that the density–embedment strength relationships still hold after the treatment despite the decrease in density and the increase in embedment strength parallel to the grain. However, after thermal modification, the influence of load direction on embedment strength was ~30% larger and the influence of calculation method (yield versus ultimate strength) on embedment strength perpendicular to the grain was ~10% smaller.

## 1. Introduction

Thermal modification is a process to improve wood's biological resistance and dimensional stability. This technology is currently commercially available throughout Europe. However, the use of thermally modified timber (TMT) is limited to non-structural applications because of the loss in strength and ductility due to the treatment, specifically in loading situations that include tensile stresses. Nevertheless, in a recent study it was shown that reasonable levels of bending strength remain after thermal modification of spruce timber, which could be predicted with sufficient accuracy [36]. Since TMT is more brittle than unmodified timber, the steel in connections can be key in introducing a ductile behaviour into the design of a load bearing structure of TMT. Examples of such structures would be outdoor playground/gym equipment and the substructure supporting outdoor decks. To be able to design these connections, more knowledge is required about the influence of thermal modification on embedment strength.

## 2. Background

The embedment strength ( $f_h$ ), besides the type of fastener and the joint's geometry, is of major importance for calculation of the load-carrying capacity of timber joints with dowel-type fasteners loaded in shear [38,8]. For common hardwood and softwood species, the embedment strength can be determined with empirical formulas, which take into account the influence of wood density, dowel diameter and load direction with respect to the fibre direction [11]. The embedment strength can also be obtained from tests, which is especially relevant when embedment properties of a certain timber are not covered by design or material standards, such as for TMT, but are required for the design. For this purpose, two tests standards are commonly used: the American standard, ASTM D 5764-97a [2], and; the European standard, EN 383 [9]. An essential difference between these standards is that ASTM D 5764-97a allows for both a half-hole and a full-hole test specimen, while EN 383 prescribes a test specimen with a full hole. When the specimen is loaded parallel to the grain according to these standards,

\* Corresponding author.

E-mail address: [joran.van.blokland@slu.se](mailto:joran.van.blokland@slu.se) (J. van Blokland).

<https://doi.org/10.1016/j.conbuildmat.2021.125517>

Received 30 April 2021; Received in revised form 26 October 2021; Accepted 31 October 2021

Available online 14 November 2021

0950-0618/© 2021 The Author(s). Published by Elsevier Ltd. This is an open access article under the CC BY license (<http://creativecommons.org/licenses/by/4.0/>).

Notations			
<b>Abbreviations</b>			
CI	Confidence interval	$f_h$	Embedment strength
DIC	Digital image correlation	$f_{h,u}$	Embedment strength at $F_u$
EC5	Eurocode 5	$f_{h,y}$	Embedment strength at $F_y$
LVDT	Linear variable differential transformer	$N$	Number of specimens
MC	Moisture content	$p$	P-value significance
RH	Relative humidity	$t$	Thickness of specimen
SEE	Standard error of the estimate	$R^2$	Coefficient of determination
TM	Thermally modified	$u$	Crosshead displacement
TMT	Thermally modified timber	$w$	Relative displacement relative displacement between the dowel and the unloaded wood close to the dowel
<b>Symbols</b>		$w_0$	Displacement at zero $F$ from extrapolating the slope of the $F-w$ curve between 20-30% of $F_{max,est}$
$\rho$	Density	$w_6$	Displacement at 60% of $F_{max,est}$ corrected with $w_0$
$\rho$	Air-dry density	$w_8$	Displacement at 80% of $F_{max,est}$ corrected with $w_0$
$\rho_{OD}$	Oven-dry density	$w_u$	Displacement at $F_u$ corrected with $w_0$
$d$	Dowel diameter	$w_y$	Displacement at $F_y$ corrected with $w_0$
$F$	Force measured by crosshead	$K_e$	Elastic foundation modulus
$F_{max,est}$	Estimated maximum load	$K_{e-}$	Elastic foundation modulus from unloading
$F_u$	Ultimate strength	$K_{e+}$	Elastic foundation modulus from reloading
$F_y$	Yield strength	$K_s$	Initial foundation modulus

there is a risk of tensile failure perpendicular to grain, i.e. splitting of the specimen, before embedment strength is reached. For this reason, ASTM D 5764-97a recommends the use of a full-hole test specimen as an alternative to one with a half-hole for species that tend to split before completion of the test. A more effective way to prevent splitting are various types of reinforcement, which were investigated by others such as Lederer et al. [22] for spruce wood specimens in a half-hole test. This approach assures that the embedment strength will be governed by embedment failure and not by tensile failure perpendicular to the grain without affecting embedment strength test values [31], and thus looks promising for wood products sensitive to splitting such as TMT.

Mechanical properties can change considerably due to thermal modification. The degree of this change depends on process parameters, mainly treatment temperature and duration, properties of the raw material, and loading type and direction [20,39,29,24,16]. The resistance to crack initiation and propagation along the grain of spruce wood decreased by approximately 50–80% due to thermal modification [27,25]. This illustrates the increased risk of splitting failure during embedment tests parallel to the grain as a result of the treatment. Splitting, instead of embedment failure, may not only cause a large scatter in test data, but also leads to an underestimation of the embedment strength of TMT. The mechanical property that strongly determines embedment strength is the compressive strength of the wood around the dowel [33]. The compressive strength parallel to the grain was found to increase between 10 and 45% due to thermal modification, whereas for the compressive strength perpendicular to the grain a decrease of 25–40% has been reported [4,40,39,12]. The stiffness found in compression tests parallel to the grain increased about 30% after thermal modification of beech wood, and about 15% in compression tests perpendicular to the grain [39,12]. In line with these results, the embedment strength of screws (4.5 mm in diameter) installed without predrilling in unmodified and thermally modified spruce wood tested according to EN 383 in the parallel to grain mode was approximately 40% higher for the treated material [6]. The above results were obtained when unmodified and modified samples were conditioned at the standard reference climate of 20 °C and 65% relative humidity (RH), which led to moisture contents between 7–14% and 3–7%, respectively. This decrease in equilibrium moisture content is mainly related to the loss in hygroscopic hemicelluloses due to the treatment [29]. This in part explains why despite the degradation of wood polymers some mechanical

properties of TMT exceed those of unmodified timber when the material is exposed to a similar climate [1]. Indeed, thermal modification had no effect on compressive strength and stiffness values when ash wood's moisture content was similar between the study and control group (~3%) [28]. The effect of moisture content on mechanical properties of unmodified wood has been studied extensively [14,15], however, for thermally modified wood, such knowledge is limited.

The embedment stiffness and strength values are also influenced by test specimen configuration. In the half-hole test, a uniform compressive load is applied over the dowel's length; whereas in the full-hole test, a compressive load is applied at the dowel's protruding ends. The half-hole test precludes dowel bending, while the full-hole test according to EN 383 aims to limit dowel bending by using fixed supports and a low specimen thickness/dowel diameter ( $t/d$ ) ratio. For example, a  $t/d$ -ratio of 2 has been recommended for this test setup [38]. Dowel bending together with gauge points for displacement influence the stiffness obtained from embedment tests, i.e. the foundation modulus  $K$  [38]. EN 383 instructs how to obtain  $K$  and how to measure local displacement, i.e. the relative displacement between the dowel and the unloaded wood close to the dowel, whereas ASTM D 5764-97a that does not include  $K$ , instructs to measure global displacement, i.e. the relative displacement between the crosshead and base plate. Previous studies that evaluate the influence of test specimen configuration (full hole versus half hole) on  $K$ , measured only global displacement [32,13]. The test specimen configuration, full hole according to EN 383 versus half hole according to ASTM D 5764-97a, had no clear effect on  $f_h$  values [32]. In contrast, a 20% difference was found when the full-hole setup had a higher  $t/d$ -ratio of 3.3, and—in line with the ASTM D 5764-97a—the dowel was simply supported instead of fixed [13]. Values of  $f_h$  also depend on the calculation method of test results. ASTM D 5764-97a uses the yield strength to calculate  $f_h$ , which is obtained by the 5% offset method, whereas EN 383 utilises the ultimate strength, which is defined as the maximum strength found before reaching 5 mm displacement. This leads in particular to disagreements for the perpendicular to grain loading situation, where the load typically increases after the yield point [33]. Other differences between the two test standards relate to specimen dimension and loading procedure. An overview of these differences as well as similarities was given by Franke and Magnière [13]. In addition,  $f_h$  is known to be influenced by the following parameters: wood density, species and moisture content; load direction and type, and; dowel diameter, surface

quality and hole size [8,31]. Although less data is available on  $K$ , it seems reasonable to assume that it is influenced by some of the parameters similar to the ones listed for  $f_h$ .

2.1. Scope

This study investigates the effect of thermal modification on the embedment properties of spruce timber. The influence of the following parameters on embedment properties are included: density (embedment strength versus density), load direction (parallel versus perpendicular to grain), test specimen configuration (half hole versus full hole), moisture content (service class 1 versus 2), gauge points (local versus global displacement) and calculation method (yield versus ultimate strength). The test specimens loaded parallel to the grain are reinforced to prevent splitting of the wood. The study is limited to one thermal modification process, one type of dowel (diameter, quality, and hole size), one wood species and two specimen dimensions (thickness, and end and edge distances); one for each load direction. The results provide new information on embedment properties of thermally modified spruce timber and a better understanding of the influence of the investigated parameters on embedment stiffness and strength values obtained from tests for both unmodified and thermally modified spruce.

3. Materials and methods

3.1. Preparation of specimens

For this study, 16 boards with cross-sectional dimensions of  $45 \times 145 \text{ mm}^2$  were sawn from eight Norway spruce (*Picea abies* [L.] Karst.) logs using a 2X-log sawing pattern; two ‘mirror imaged’ boards per log (Fig. 1). These boards were picked from a larger batch, while it was ensured that a range of densities was covered. The average and standard deviation values of air-dry density (at  $\sim 20 \text{ }^\circ\text{C}/60\% \text{ RH}$ ) of board pairs cut from logs 1–8 was  $456 \pm 32 \text{ kg m}^{-3}$ . Eight boards (i.e. one from each log) were thermally modified according to the ThermoWood® process to meet class Thermo-D (max.  $212 \text{ }^\circ\text{C}/3 \text{ h}$ ) [18]. Detailed information on the selection of timber and modification process can be found in van Blokland et al. [37]. Specimens cut from thermally modified (TM) boards are referred to as ‘TM spruce’, whereas specimens cut from unmodified boards served as a reference and are referred to as ‘spruce’. Specimens were prepared according to EN 383 [9] and ASTM D 5764-97a (2013), and their dimensions, and end and edge distances are shown in Fig. 1 and Fig. 3. The wood around the dowel hole was knot-free. Other parts of the specimen could contain knots, which was typical for specimens 400 mm in length. A 10 mm diameter hole was made in each test specimen to fit a steel dowel. The steel dowel had a turned, ground and polished shaft with a diameter ( $d$ ) of 10 mm, and belonged to strength class 8.8 [10]. In total, two matched specimens of each dimension were obtained per board; one was conditioned at  $20 \text{ }^\circ\text{C}/65\% \text{ RH}$  and one at  $20 \text{ }^\circ\text{C}/85\% \text{ RH}$  (Fig. 1). These climate conditions correspond to respective service classes 1 (indoor environment) and 2

(outdoor aboveground, but not exposed to the weather) as defined by EN 1995-1-1 [11], i.e. Eurocode 5 (EC5), a standard used for the design of timber structures. Service class 3 conditions (outdoor aboveground, and exposed to the weather) are not included. The number of specimens ( $N$ ) included was 128 for a total of 16 test series, i.e. 8 specimens per test series. Each series is determined by test specimen configuration (full hole or half hole), load direction (parallel or perpendicular to the grain), treatment level (unmodified or thermally modified) and moisture level (conditioned at  $20 \text{ }^\circ\text{C}/65\% \text{ RH}$  or  $20 \text{ }^\circ\text{C}/85\% \text{ RH}$ ). Dowel properties, which can have a considerable effect on  $f_h$  [31], were not determined, but only one dowel type was used.

3.2. Embedment tests

All 128 specimens were loaded displacement-controlled in compression using a MTS-810 testing machine (MTS Systems Corporation, Eden Prairie, MN), while force,  $F$  [kN], and crosshead displacement,  $u$  [mm], were recorded. Local displacement,  $w$  [mm], was measured by two linear variable differential transformers (LVDTs) according to EN 383. The LVDTs have a measuring accuracy of 0.001 mm and were mounted to the load fixture, one at each dowel end (Fig. 2).

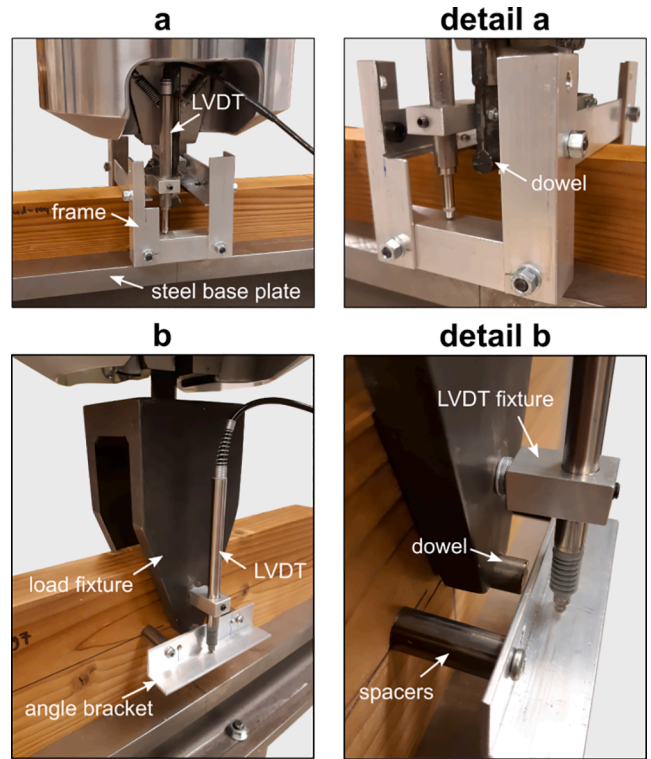


Fig. 2. Position of LVDTs during a half-hole and b full-hole tests.

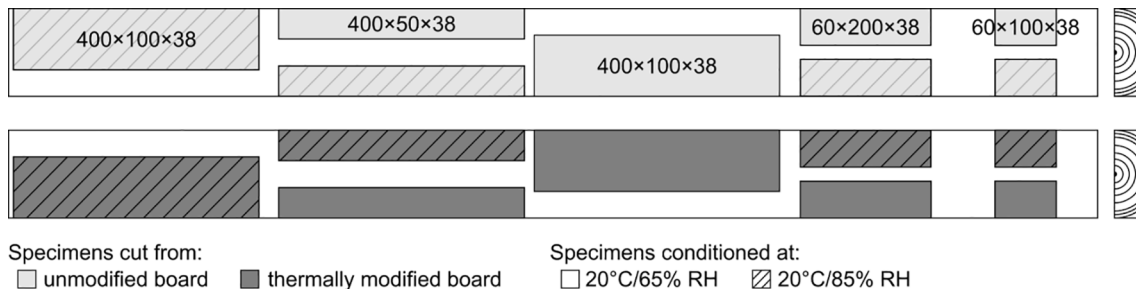


Fig. 1. Preparation of specimens. Note that unmodified and thermally modified board pairs were cut from the same part of the log and dimensions are given in millimetres.

During half-hole tests, an aluminium frame was placed on top of the specimen and fixed with two screws; one screw at either side of the dowel at a distance of  $3d$ . Local displacement was measured in a similar manner during full-hole tests, but this time with two angle brackets, one at each side of the specimen (Fig. 2).  $w$  was taken as the average of both LVDT readings. The gauge points used for local displacement are shown in Fig. 3. In addition, one digital image correlation (DIC) measurement was made on specimens cut from one log (see Section “DIC measurements”). For these 16 specimens, local displacement was not recorded in order to maintain maximum field of view during DIC measurements.

After 0.3 kN preloading, tests were performed at a  $1 \text{ mm min}^{-1}$  displacement rate and included one unloading–reloading cycle between 10 and 40% of the estimated maximum load,  $F_{\text{max,est}}$ . Based on

preliminary tests on both TM spruce and spruce, the maximum load was estimated at 10 kN for parallel to grain loading and 6 kN for perpendicular to grain loading. Before unloading, the crosshead displacement was held constant for 30 sec to minimize the influence of time-dependent effects on the displacements measured during unloading. The test was terminated after reaching 5 mm local displacement. This loading procedure was in line with EN 383 but deviated from ASTM D 5764-97a, because of the unloading–reloading cycle that is not included in that standard. The cycle was included to obtain the elastic embedment stiffness,  $K$ , but at the expense of slightly conservative  $f_h$  values [38]. For half-hole tests, a 4 mm steel plate of quality S 355 was welded to the dowel to apply the load. For full-hole tests, a loading fixture of steel quality S 355 was used to apply load on top of the dowel’s protruding ends. A 1.5 mm clearance between the fixture and the specimen was provided on either side. The full-hole setup allowed to study the displacement field around the dowel with DIC. The setup was as prescribed by ASTM D 5764-97a, but deviated from EN 383 because the dowel was simply supported instead of fixed. Because of these support conditions and the  $t/d$  ratio of 3.8 (EN 383 recommends  $1.5 \leq t/d \leq 4$ ), elastic dowel bending during testing should be substantial in this full-hole setup.

To prevent splitting upon loading parallel to the grain, reinforcement was applied at a distance of  $3d$  under the dowel by means of two 3 mm thick aluminium plates of  $40 \times 60 \text{ mm}^2$  that were connected using a 4 mm threaded rod through the centre of the specimen, ring washers and nuts (Fig. 3). Tightening was done manually and avoided pre-tensioning.

The mass and volume of the entire specimens were taken at the time of testing, and again after oven-drying specimens for at least 24 h at  $103 \text{ }^\circ\text{C}$  until the change in mass was  $<0.1\%$  per 2 h.

### 3.3. DIC measurements

A DIC system (Aramis adjustable, GOM GmbH, Germany) that runs Aramis™ software (GOM Correlate, GOM Software 2018) was used to obtain surface strains on one side of the specimen during testing. The surface of these specimens was prepared with a speckle pattern to provide camera images with the necessary grey scale information. The measuring area of the two cameras was  $180 \times 140 \text{ mm}^2$  with a full frame resolution of  $4096 \times 3072$  pixels. Here a facet size of  $19 \times 19$  pixels at a distance of 15 pixels was used. The engineering strain computed by the Aramis™ software was therefore calculated over a length of approximately 1.2 mm. During tests, images were taken at a frequency of 0.5 Hz. For the displacement rate of  $1 \text{ mm min}^{-1}$ , this corresponded to a load step of about 0.03 mm between each frame. DIC enabled to study the effect of treatment, test specimen configuration and moisture content on strain development and to identify failure modes (see Section “Failure modes”). The distinction between the different failure modes was based on a visual inspection of the tested specimens and a comparison made with the obtained strain profiles through DIC.

### 3.4. Calculation of properties

Fig. 4 shows the properties that were determined from the recorded load–displacement curves. The initial foundation modulus,  $K_s$  [ $\text{N mm}^{-3}$ ], was calculated as the slope between 20 and 30% of  $F_{\text{max,est}}$  divided by the product of  $d$  and  $t$ , where  $t$  is the thickness of the specimen ( $\sim 38 \text{ mm}$ ). The elastic foundation modulus,  $K_e$  [ $\text{N mm}^{-3}$ ], was calculated in a similar manner as  $K_s$ , but by using the slopes of the unloading–reloading cycle.  $K_e$ , calculated from the slope of unloading, is denoted as  $K_{e-}$ , and  $K_{e+}$  was determined from the slope of reloading (Fig. 4, detail K). Since tests were displacement controlled,  $F$  decreased during the holding phase from 40% of  $F_{\text{max,est}}$  to about 30–35% of  $F_{\text{max,est}}$  due to relaxation. In addition, non-linearity is typically observed in the last part of unloading, which was between 10 and 20% of  $F_{\text{max,est}}$  in our study [34]. Therefore, the first part of unloading was used to obtain  $K_{e-}$  instead of the usual interval, which is between 10 and 40% of  $F_{\text{max,est}}$

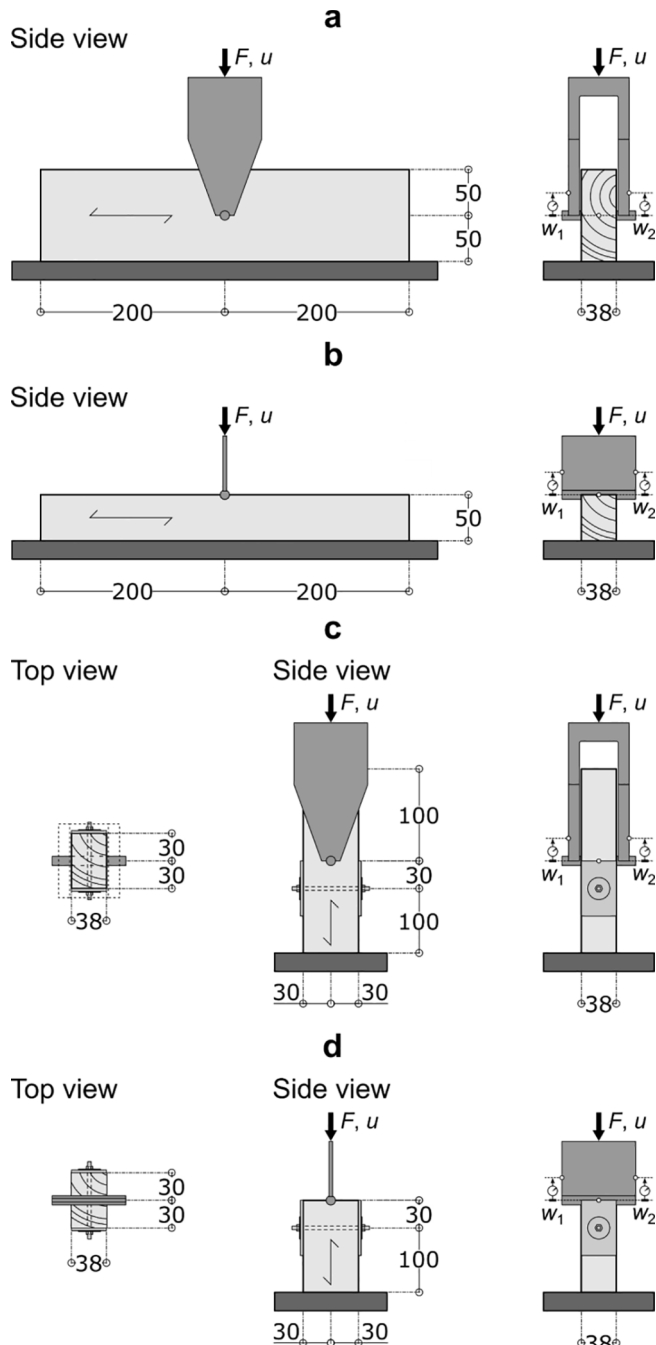


Fig. 3. Test setup of a the full-hole and b the half-hole test for perpendicular to grain loading, and c the full-hole and d the half-hole test for parallel to grain loading. Dimensions in millimetres.

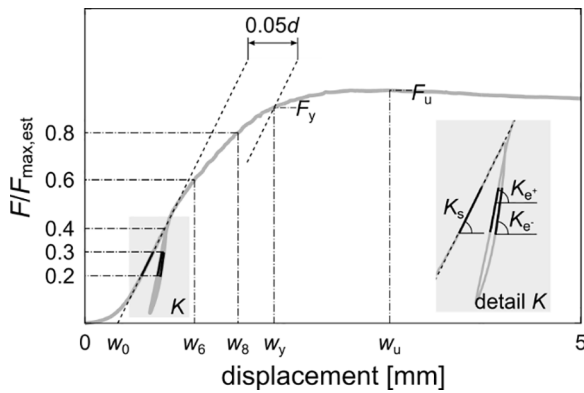


Fig. 4. Properties obtained from load–displacement curve. Note that in this example no corrections with  $w_0$  were made.

[9]. Consistently, the same load levels (20–30% of  $F_{max,est}$ ) were used to obtain  $K_s$  and  $K_e$ . The intersection of the load–displacement curve and the “5% offset line” was used to determine the yield strength,  $F_y$  [kN], and the corresponding yield displacement,  $w_y$  [mm]. The 5% offset line was obtained from the slope  $K_s$ , which was shifted by a displacement equal to 0.05 times  $d$  (Fig. 4). The maximum load during tests defines the ultimate strength,  $F_u$  [kN], and the corresponding ultimate displacement,  $w_u$  [mm]. The embedment strengths [MPa] at yielding and ultimate load were calculated as  $f_{h,y} = F_y/(d \cdot t)$  and  $f_{h,u} = F_u/(d \cdot t)$ , respectively. The displacement [mm] at 60% ( $w_6$ ) and 80% ( $w_8$ ) of  $F_{max,est}$  were recorded in order to assess possible effects of the investigated parameters on the shape of the load–displacement curve. The derivation of the above properties is in line with ASTM D 5764-97a and EN 383 standards. Furthermore, displacements  $w_6$ ,  $w_8$ ,  $w_y$  and  $w_u$  were corrected with  $w_0$  for a better comparability between tests. Here  $w_0$  is the displacement found at zero load when extrapolating the slope  $K_s$  (Fig. 4). The embedment properties were determined from  $F-u$  curves in a similar manner as described above. Densities and moisture content were calculated from mass and volume.

### 3.5. Statistical analysis

Mean and standard deviation values of samples were calculated from individual test results (see Section “Calculation of properties”). The significance of differences in mean values of embedment properties obtained from local versus global displacement were evaluated with a dependent  $t$ -test, whereas an independent  $t$  test was used to evaluate the significance of differences in mean values of embedment properties between and within samples. Mean load–displacement curves of samples were calculated after correcting each curve individually with  $w_0$  and the inverse  $t$  distribution was used to compute a confidence interval (CI) on the mean. The results on density, moisture content and embedment properties (see Section “Results and discussion”) did not include the data obtained from specimens used for DIC. All calculations and statistics were done using the software Matlab® (Version R2018b).

## 4. Results and discussion

### 4.1. Density and moisture content

Mean and standard deviation values of density ( $\rho$ ), oven-dry density ( $\rho_{OD}$ ) and moisture content (MC) are presented in Table 1 for spruce and TM spruce and the two investigated moisture levels. Although specimens were obtained from seven logs only, the level and variation in density of samples were comparable to unmodified and thermally modified spruce timber coming from Sweden [19,37]. The average  $\rho_{OD}$  was approximately 5% lower for TM spruce than for spruce. This difference is explained by the loss in mass as a result of the treatment,

Table 1

Basic properties (mean  $\pm$  standard deviation values).

Treatment	RH	N	$\rho$	$\rho_{OD}$	MC
[–]	[%]	[no.]	[kg m <sup>-3</sup> ]	[kg m <sup>-3</sup> ]	[%]
spruce	65	28	450 $\pm$ 38	425 $\pm$ 37	12.5 $\pm$ 0.3
spruce	85	28	463 $\pm$ 37	428 $\pm$ 36	17 $\pm$ 0.4
TM spruce	65	28	419 $\pm$ 37	404 $\pm$ 36	6.2 $\pm$ 0.5
TM spruce	85	28	423 $\pm$ 36	401 $\pm$ 36	9.6 $\pm$ 0.7

mainly due to thermal degradation of hemicellulose [35,29]. The MC at the time of testing was approximately 12% for spruce conditioned at the standard reference climate, whereas under the same conditions the MC of TM spruce was only half of that (Table 1). This difference in MC between spruce and TM spruce was expected and agrees well with the decrease in equilibrium moisture content typically found after thermal modification [18,5]; mainly due to the loss in hygroscopic hemicellulose [30]. The MC of samples conditioned at 20 °C/85% RH was approximately 40% higher compared to the reference conditions for spruce and 50% higher for TM spruce, which is in accordance with results presented in the ThermoWood Handbook [18].

### 4.2. Surface strain

The strain distributions at  $u_8$  (see again Fig. 4) obtained with DIC during parallel to grain loading (i.e. for  $F \approx 8$  kN) and perpendicular to grain loading (i.e. for  $F \approx 4.8$  kN) are shown in Fig. 5 and Fig. 6, respectively. Note that subfigures in Fig. 5 and Fig. 6 display longitudinal ( $\epsilon_{xx}$ ) [left], transverse ( $\epsilon_{yy}$ ) [centre] and shear ( $\epsilon_{xy}$ ) [right] strains for full-hole (top) and half-hole tests (bottom), where the  $x$ -direction is aligned with the fibre direction. It was aimed to capture strain fields at comparable load levels. Nevertheless, comparisons of strain between tests were done at slightly different levels of loading (Fig. 5 and Fig. 6), because the increase in force around  $u_8$  varied between 65 and 375 N s<sup>-1</sup> depending on test specimen configuration and treatment level, while the logging interval of Aramis<sup>TM</sup> was 2 s.

Despite the expected difference in compressive stiffness between spruce and TM spruce, there was no obvious effect of thermal modification on the levels and distribution of strains during parallel and perpendicular to grain loading. Overall, the results shown in Fig. 5 and Fig. 6 were in line with DIC measurements of dowel embedment behaviour in Norway spruce laminated veneer lumber [34].

The magnitude and distribution of different strains found during parallel and perpendicular to grain loading were comparable between test specimen configurations (Fig. 5 and Fig. 6). However, small differences could be observed due to stress transfer around the dowel hole. For parallel to grain loading, some tensile  $\epsilon_{xx}$  were visible at both sides of the dowel hole during full-hole tests independent of treatment level, which emphasizes that part of the wood around the dowel contributes to the load transfer parallel to the grain. This way of transferring load was obviously not possible in the half-hole test setup. For the perpendicular to grain load situation some clear difference in  $\epsilon_{yy}$  (Fig. 6) were observed between full-hole and half-hole tests. In both test setups, peak  $\epsilon_{yy}$  strains of approximately –1% were found, however, these higher surface strains were spread over a much larger area in the half-hole test than the full-hole test. This may again be explained by the wood surrounding the dowel in the full-hole setup, which transferred a part of the stress in tension.

### 4.3. Failure modes

Spruce and TM spruce material directly below the dowel showed cell buckling and cell crushing due to embedment loading parallel and perpendicular to the grain, respectively, similar to earlier reports on unmodified spruce wood [21]. The brittle failure modes remained local and all specimens could be loaded up to the maximum displacement of 5

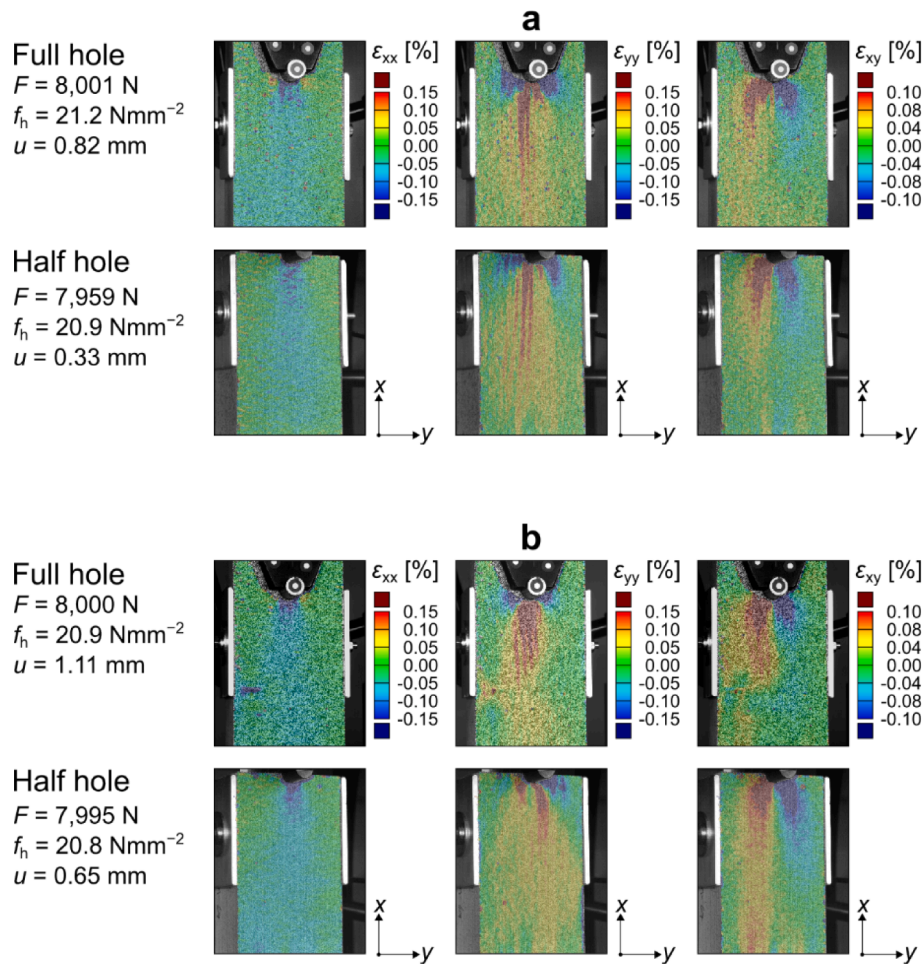


Fig. 5. Strain distribution at  $u_8$  ( $F \approx 8$  kN) during parallel to grain loading of a TM spruce and b spruce matched specimens conditioned at 20 °C/65% RH. Note that subfigures display  $\epsilon_{xx}$  (left),  $\epsilon_{yy}$  (centre) and  $\epsilon_{xy}$  (right) for half-hole tests (top) and full-hole tests (bottom), where the x-direction is aligned with the fibre direction. A colour version is available online.

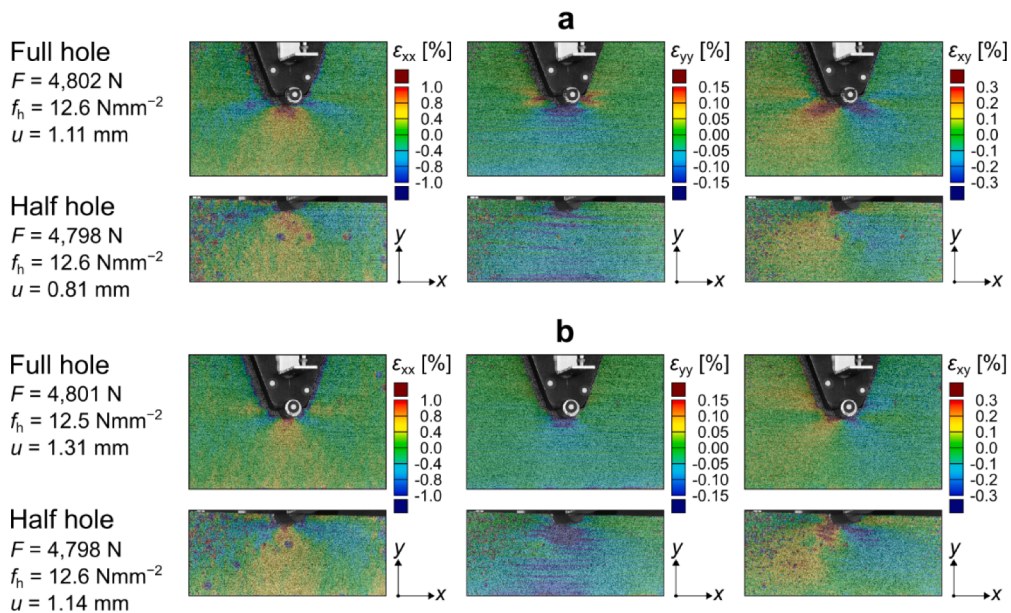


Fig. 6. Strain distribution at  $u_8$  ( $F \approx 4.8$  kN) during perpendicular to grain loading of a TM spruce and b spruce matched specimens conditioned at 20 °C/65% RH. Note that subfigures display  $\epsilon_{xx}$  (left),  $\epsilon_{yy}$  (centre) and  $\epsilon_{xy}$  (right) for full-hole tests (top) and half-hole tests (bottom), where the x-direction is aligned with the fibre direction. A colour version is available online.

mm, because failure of the entire specimen was prevented by the applied reinforcement. This was shown earlier by Lederer et al. [22] for other types of reinforcement such as screws, glued on wood-based panels and punched metal plates. In addition, four other wood failure modes were observed (Fig. 7): two for the parallel to grain load situation, namely splitting failure related to tension perpendicular to grain, shear, or a combination of the two (Fig. 7a and b), and a combined failure of shear and compression (analogue to block shear failure) (Fig. 7c), and; two for the perpendicular to grain load situation, namely shear failure (Fig. 7d), and tensile failure parallel to grain (Fig. 7d).

Splitting below the dowel hole occurred more frequently and was more substantial for TM spruce than for spruce, particularly in the half-hole test setup (100% versus 57%) (Fig. 7a). The combined failure ('block shear') was observed both for spruce and for TM spruce in tests parallel to the grain (25% and 35%, respectively) (Fig. 7c).

Unfortunately, the selected specimens that were tested with DIC did not capture this failure mode. Also, this type of failure was not observed earlier by Lederer et al. [21] for this load direction. Shear failure is common in embedment tests perpendicular to the grain and develops along the grain besides the dowel hole [21]. This failure mode was recorded for both spruce and TM spruce (Fig. 7d, top and bottom), but appeared more often in spruce (91% versus 66%). On the other hand, TM spruce loaded perpendicular to the grain failed more often in tension parallel to the grain (71% versus 36%) (Fig. 7d, centre and bottom). This difference may be explained by the decrease in tensile strength parallel to the grain due to thermal modification, which on average can be as much as 40% for commercial treatments [4,39]. Although the area above the dowel's hole was not measured by DIC, splitting above the dowel hole was observed in the full-hole test setup, but only for TM spruce (20%) (Fig. 7b). No obvious differences in failure modes between test specimen configurations were found for perpendicular to grain loading. In addition, moisture levels had no apparent effect on wood failure modes around the dowel hole.

#### 4.4. Embedment properties

Mean and standard deviation values of embedment properties are shown in Table 2 for each test series. The effect of thermal modification on the embedment behaviour is also illustrated in Fig. 8. There, mean load–displacement ( $F-w$ ) curves including 95% CIs are plotted for TM spruce and spruce loaded parallel and perpendicular to the grain and tested in the full-hole and half-hole test setup. Thermal modification had a considerable effect on the embedment strength parallel to the grain, which was higher for TM spruce than for spruce with an average difference of 27% when samples conditioned at the same climate were compared (Table 2 and Fig. 8). For this load situation, the displacement at ultimate strength,  $w_{th}$ , was 30–50% smaller after thermal modification. On the other hand, the embedment strength perpendicular to the grain decreased due to thermal modification—on average by ~ 10%. This difference was relatively small compared to the influence of the calculation method on  $f_h$  perpendicular to the grain and similar to that of moisture, as discussed below, and was often not statistically significant (Table 2). The effect of treatment on foundation moduli was somewhat ambiguous for both load directions, but overall, the results showed TM spruce tended to behave stiffer than spruce (Table 2).

The increase in  $f_h$  parallel to the grain and decrease in  $f_h$  perpendicular to the grain due to thermal modification corresponds to the degree of the effect of heat treatment on the compressive strength of wood, as discussed earlier (see Section "Background"). The change in wood chemistry due to thermal modification leads to physical changes of the wood, such as lower sorption, which, at same climatic conditions, results in a lower moisture content of TM spruce compared to spruce (see Section "Density and moisture content"). The results show that the difference in  $f_h$  parallel to the grain was only 5% on average when comparing spruce conditioned at 65% RH versus TM spruce conditioned at 85% RH (i.e. when  $\Delta MC$  was only ~ 3% between sample sets). Thus, for tests parallel to the grain conducted under specific climatic conditions, a large share of the increase in embedment strength due to thermal modification can be explained by the change in the physical properties, i.e. the decrease in equilibrium moisture content. On the other hand, the decrease in  $f_h$  perpendicular to the grain due to thermal modification is mainly a result of the degradation of wood polymers, since, at similar climatic conditions, the MC was lower in TM spruce than spruce (Table 1). In detail, when only considering the difference in MC between spruce and TM spruce conditioned at 65% RH, an increase in  $f_h$  of 19–25% was expected [14,17]. Instead, the decrease in  $f_h$  points out the important role hemicelluloses have on the compressive strength perpendicular to the grain. Previously, it was shown the critical role of this wood constituent on stiffness in compression [3].

In the following sections, the influence of thermal modification on embedment properties in relation to the investigated parameters are

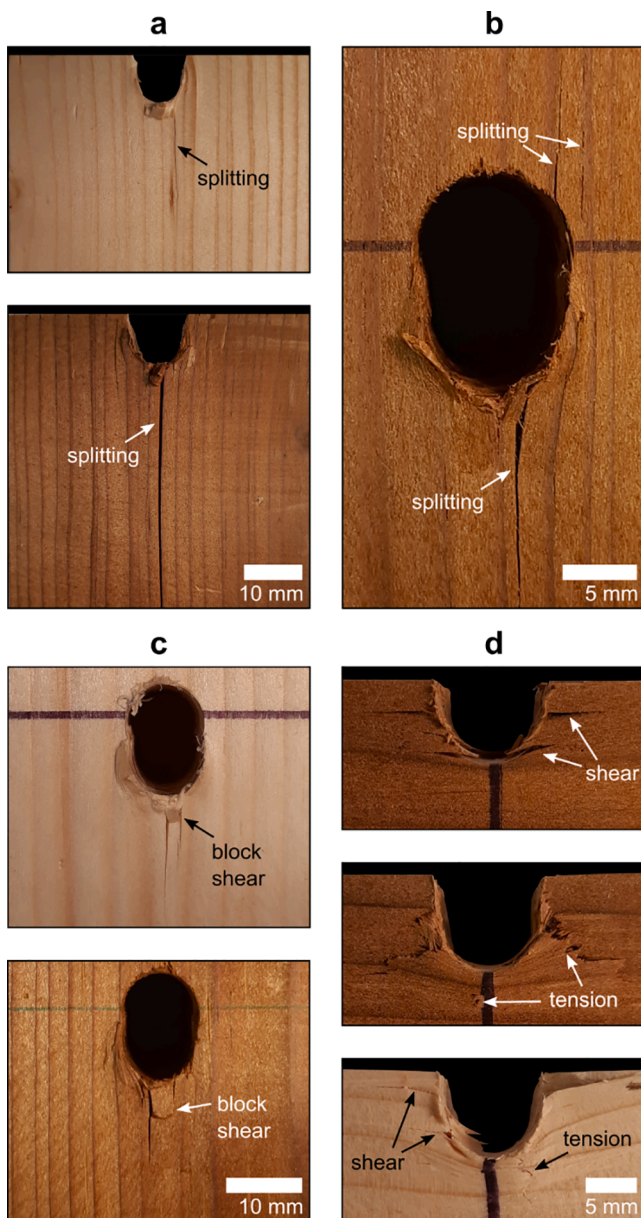


Fig. 7. Examples of failure modes: a splitting failure, b splitting failure above dowel hole and c block failure from parallel to grain loading, and d shear failure (top), tension failure (middle), and shear and tension failure (bottom) from perpendicular to grain loading. Note that subfigures display failure modes for spruce (light-coloured wood) and TM spruce (dark-coloured wood).

**Table 2**  
Embedment properties (mean ± standard deviation values) from local displacement (*w*)

Treatment [-]	RH [%]	Stiffness [N mm <sup>-3</sup> ]			Displacement [mm]				Strength [N mm <sup>-2</sup> ]	
		<i>K<sub>s</sub></i>	<i>K<sub>e</sub></i>	<i>K<sub>e'</sub></i>	<i>w<sub>6</sub></i>	<i>w<sub>8</sub></i>	<i>w<sub>y</sub></i>	<i>w<sub>u</sub></i>	<i>f<sub>h,y</sub></i>	<i>f<sub>h,u</sub></i>
<b>PARALLEL TO GRAIN</b>										
Full-hole test										
Spruce	65	26 ± 3 <sup>a,b,c</sup>	61 ± 8 <sup>a,b</sup>	50 ± 4 <sup>a,b</sup>	0.6 ± 0.1 <sup>a,c,b</sup>	0.9 ± 0.2 <sup>a,b,c</sup>	1.7 ± 0.2 <sup>a,c</sup>	3 ± 0.5 <sup>a,b,c,d</sup>	29 ± 5 <sup>b,c,D</sup>	32 ± 4 <sup>b,c</sup>
Spruce	85	15 ± 2 <sup>a,b,c,d</sup>	65 ± 10 <sup>a,b</sup>	47 ± 4 <sup>a,b</sup>	1.1 ± 0.2 <sup>a,c,d</sup>	1.8 ± 0.3 <sup>a,b,c,d</sup>	2.1 ± 0.4 <sup>a,b,c</sup>	4.1 ± 0.7 <sup>a,c,d</sup>	23 ± 3 <sup>b,c,d</sup>	26 ± 3 <sup>b,c,d</sup>
TM spruce	65	23 ± 4 <sup>A,b</sup>	62 ± 11 <sup>a,b</sup>	49 ± 4 <sup>a,b</sup>	0.7 ± 0.1 <sup>a,B</sup>	0.9 ± 0.1 <sup>a,B,C</sup>	2.1 ± 0.4 <sup>a,b</sup>	2.1 ± 0.2 <sup>a,b,d</sup>	37 ± 5 <sup>b,D</sup>	37 ± 5 <sup>b</sup>
TM spruce	85	20 ± 5 <sup>a,b,D</sup>	59 ± 6 <sup>a,b</sup>	47 ± 4 <sup>a,b</sup>	0.8 ± 0.2 <sup>a,d</sup>	1.2 ± 0.3 <sup>a,B,C,d</sup>	2.1 ± 0.4 <sup>a,b</sup>	2.5 ± 0.4 <sup>a,b,d</sup>	32 ± 5 <sup>b,d</sup>	33 ± 4 <sup>b,d</sup>
Half-hole test										
Spruce	65	49 ± 12 <sup>a,b</sup>	196 ± 14 <sup>a,b,D</sup>	151 ± 15 <sup>a,b</sup>	0.4 ± 0.1 <sup>a,B</sup>	0.6 ± 0.2 <sup>a,c,D</sup>	1.1 ± 0.1 <sup>a</sup>	2.1 ± 0.4 <sup>a,b,c,d</sup>	31 ± 4 <sup>b,c,d</sup>	34 ± 5 <sup>b,c,D</sup>
Spruce	85	39 ± 10 <sup>a,b</sup>	194 ± 11 <sup>a,b</sup>	139 ± 12 <sup>a,b</sup>	0.5 ± 0.1 <sup>a,b</sup>	0.9 ± 0.2 <sup>a,b,c,D</sup>	1.1 ± 0.2 <sup>a,d</sup>	2.9 ± 0.3 <sup>a,b,c,d</sup>	24 ± 2 <sup>b,c,d</sup>	29 ± 3 <sup>b,c,d</sup>
TM spruce	65	65 ± 32 <sup>A,B</sup>	229 ± 31 <sup>a,b,D</sup>	182 ± 26 <sup>a,b</sup>	0.3 ± 0.1 <sup>a,b,c</sup>	0.4 ± 0.1 <sup>a,b,c,D</sup>	1.2 ± 0.3 <sup>a</sup>	1.1 ± 0.2 <sup>a,b,c,d</sup>	41 ± 5 <sup>b,c,d</sup>	41 ± 5 <sup>b,c,D</sup>
TM spruce	85	35 ± 8 <sup>a,b</sup>	211 ± 44 <sup>a,b</sup>	154 ± 30 <sup>a,b</sup>	0.5 ± 0.1 <sup>a,c</sup>	0.7 ± 0.2 <sup>a,b,c,D</sup>	1.5 ± 0.2 <sup>a,b,d</sup>	1.6 ± 0.3 <sup>a,b,c,d</sup>	33 ± 3 <sup>b,c,d</sup>	33 ± 3 <sup>b,c,d</sup>
<b>PERPENDICULAR TO GRAIN</b>										
Full-hole test										
Spruce	65	13 ± 2 <sup>a,b,c</sup>	28 ± 2 <sup>a,b</sup>	25 ± 2 <sup>a,b</sup>	0.8 ± 0.1 <sup>a,b,c</sup>	1.6 ± 0.5 <sup>B,c</sup>	1.6 ± 0.2 <sup>a,D</sup>	4.7 ± 0.2 <sup>A,b</sup>	13 ± 1 <sup>b,c,D</sup>	20 ± 2 <sup>b</sup>
Spruce	85	11 ± 1 <sup>a,b,c</sup>	29 ± 2 <sup>a,b</sup>	26 ± 2 <sup>a,b</sup>	1.1 ± 0.2 <sup>c</sup>	2.5 ± 0.5 <sup>b,c</sup>	1.6 ± 0.1 <sup>B,D</sup>	4.7 ± 0.1 <sup>a</sup>	11 ± 1 <sup>b,c</sup>	17 ± 2 <sup>b,d</sup>
TM spruce	65	14 ± 2 <sup>a,b,c</sup>	29 ± 2 <sup>a,b</sup>	27 ± 2 <sup>a,b</sup>	0.9 ± 0.2 <sup>a,B</sup>	2.2 ± 1.1 <sup>B</sup>	1.4 ± 0.1 <sup>a,b,D</sup>	4.8 ± 0 <sup>b</sup>	12 ± 1 <sup>b,D</sup>	18 ± 4 <sup>b</sup>
TM spruce	85	12 ± 2 <sup>A,b,c</sup>	28 ± 3 <sup>a,b</sup>	26 ± 3 <sup>a,b</sup>	1.2 ± 0.6	2.8 ± 1 <sup>*a,B</sup>	1.4 ± 0.1 <sup>a,b,D</sup>	4.8 ± 0.1 <sup>b</sup>	11 ± 1 <sup>b</sup>	14 ± 2 <sup>b,d</sup>
Half-hole test										
Spruce**	65	21 ± 2 <sup>a,b</sup>	45 ± 5 <sup>a,b</sup>	40 ± 4 <sup>a,b</sup>	0.6 ± 0.1 <sup>a,B,c</sup>	1.3 ± 0.8	1.2 ± 0.1 <sup>a</sup>	4.9 ± 0 <sup>A,b</sup>	14 ± 2 <sup>b</sup>	21 ± 4 <sup>b</sup>
Spruce	85	15 ± 5 <sup>a,b</sup>	42 ± 6 <sup>a,b</sup>	36 ± 5 <sup>a,b</sup>	0.9 ± 0.3 <sup>b,c</sup>	2.0 ± 0.9 <sup>B</sup>	1.3 ± 0.3	4.9 ± 0.1 <sup>a,b</sup>	12 ± 2 <sup>b</sup>	19 ± 2 <sup>b,D</sup>
TM spruce**	65	23 ± 3 <sup>a,b,c</sup>	50 ± 7 <sup>a,b</sup>	44 ± 5 <sup>a,b</sup>	0.5 ± 0.1 <sup>a,b</sup>	1.2 ± 0.6 <sup>B</sup>	1.1 ± 0.1 <sup>a</sup>	4.9 ± 0.1 <sup>b</sup>	14 ± 2 <sup>b,c</sup>	19 ± 4 <sup>b</sup>
TM spruce	85	19 ± 5 <sup>A,b,c</sup>	47 ± 7 <sup>a,b</sup>	42 ± 7 <sup>a,b</sup>	0.9 ± 0.5	2.2 ± 1.1 <sup>*a,B</sup>	1.1 ± 0.1 <sup>a,b</sup>	4.9 ± 0.1 <sup>b</sup>	11 ± 2 <sup>b,c</sup>	15 ± 2 <sup>b,D</sup>

Sample size: \**N* = 6, \*\**N* = 5, otherwise *N* = 7.

Statistical test: independent *t*-tests for differences in mean values.

<sup>a,A</sup>Significance full hole vs. half hole test.

<sup>b,B</sup>Significance parallel vs. perpendicular to grain loading.

<sup>c,C</sup>Significance 65% vs. 85% RH.

<sup>d,D</sup>Significance spruce vs. TM spruce.

Significance levels: lower case letters *p* < 0.01 (e.g. a), upper case letters *p* < 0.05 (e.g. A)

discussed in depth.

#### 4.5. Influence of density: embedment strength versus density

The relationships between density and embedment strength (*f<sub>h,u</sub>*) are shown in Fig. 9 for spruce and TM spruce, and for parallel and perpendicular to grain loading (results from full-hole and half-hole tests are combined in this figure). The figure also includes the  $\rho$ -*f<sub>h,u</sub>* relationships as given by EC5 (Expressions 8.31–33) for unmodified softwoods (red dash-dotted line). The expressions given by EC5 are mean curves based on experimental data, which are used to obtain a characteristic value of *f<sub>h,u</sub>* based on the characteristic density [23]. The *f<sub>h,u</sub>* values of spruce that were found in this study are consistent with the expressions used in EC5, and *f<sub>h,u</sub>* increases with density,  $\rho$ , as expected. Fig. 9 shows, for both load situations, that the  $\rho$ -*f<sub>h,u</sub>* relationships hold after the treatment despite the decrease in density and the increase in *f<sub>h,u</sub>* parallel to the grain (see also Table 1 and Table 2). The observed effect of thermal modification on the  $\rho$ -*f<sub>h,u</sub>* relationship from tests parallel to the grain is consistent with a previous study on screw-type fasteners [6]. The overestimation of the EC5 formula for unmodified timber with densities below ~ 450 kg m<sup>-3</sup>, as seen in Fig. 9 for both load directions, was observed earlier on a much larger data set [31].

#### 4.6. Influence of load direction: parallel versus perpendicular to grain

The embedment behaviour of unmodified wood strongly depends on

load angle with respect to the direction of the grain [9]. In line with our expectations (see Section “Background”), large differences between the load situations parallel and perpendicular to the grain were also found for TM spruce, both for foundation moduli and embedment strength values (Table 2 and Fig. 8). For all test series, *K<sub>s</sub>*, *K<sub>e</sub>*, *f<sub>h,y</sub>* and *f<sub>h,u</sub>* were found to be 27–65%, 45–78%, 50–68% and 34–57% lower for tests perpendicular to the grain compared to those parallel to the grain, respectively. These differences in strength values are consistent with Sawata and Yasumua [33], who also showed that for *f<sub>h,u</sub>* these differences are dowel diameter dependent. However, load direction had a larger effect on the embedment strength of TM spruce than for spruce, with an average difference between the parallel and perpendicular loading direction of 61% versus 45%, respectively, whereas no such difference was found for the embedment stiffness (Table 2). This larger difference seen between load directions for TM spruce directly follows from the increase in *f<sub>h</sub>* parallel to grain and decrease in *f<sub>h</sub>* perpendicular to grain due to thermal modification, discussed earlier (beginning of Section “Embedment properties”).

#### 4.7. Influence of test specimen configuration: half hole versus full hole

The largest differences in embedment properties as a result of test specimen configuration were found for the initial (*K<sub>s</sub>*) and elastic (*K<sub>e</sub>*) foundation modulus parallel to the grain, which were 80–180% and 200–280% higher when determined in the half-hole compared to the full-hole test setup, respectively (Table 2). The half-hole setup also

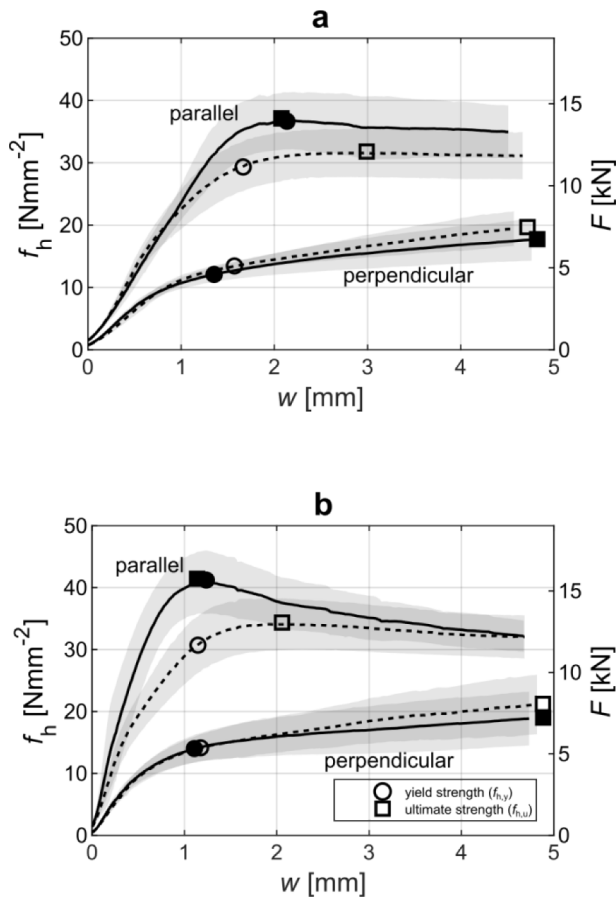


Fig. 8. Mean load–displacement curves including 95% CIs of TM spruce (solid lines/filled markers) and spruce (dashed lines/non-filled markers) samples conditioned at 65% RH loaded in the a full-hole and b half-hole test setup. Legend given in b.

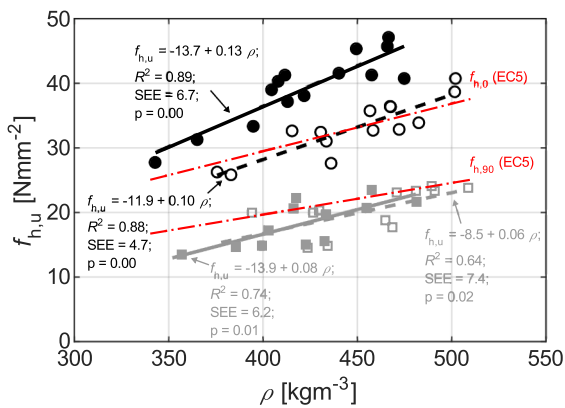


Fig. 9. Scatter plot of  $\rho$  versus  $f_{h,u}$  for spruce (non-filled symbols) and TM spruce (filled symbols) conditioned at 65% RH loaded parallel (black circles) and perpendicular (grey squares) to the grain. Included are regression lines per sample with corresponding coefficient of determination ( $R^2$ ), standard error of the estimate (SEE) and significance ( $p$ -value), and  $\rho$ – $f_{h,u}$  relationships from EC5 (red dash-dotted lines) for loading parallel ( $f_{h,u}$ ) and perpendicular ( $f_{h,u,90}$ ) to the grain. A colour version is available online.

resulted in considerably higher values of  $K_s$  and  $K_e$  perpendicular to the grain, but these differences were smaller (40–70%). It was observed that, on average, these differences were larger for TM spruce than for spruce (217% versus 178% for parallel and 64% versus 51% for perpendicular to grain loading), but the results were somewhat

ambiguous. No such difference was found for the embedment strength (on average, 7% for TM spruce and 8% for spruce). In agreement with previous results [32,13], the results in Table 2 confirm that test specimen configuration, half-hole or full-hole, has a relatively small and not statistically significant effect on the embedment strength. Nevertheless,  $f_{h,y}$  and  $f_{h,u}$  typically were higher when determined in the half-hole test setup, and on average this difference was 7%. Fig. 10 shows the influence of test setup on mean  $F$ – $w$  curves for both load situations.

The large differences in stiffness between the two test specimen configurations mainly are a consequence of the deflection of the dowel upon testing, which was precluded in the half-hole setup (dowel supported over full length by steel plate), whereas free rotation was possible in the full-hole setup (dowel simply supported at ends by fixture), as discussed earlier (Sections “Background” and “Embedment tests”). In a previous study, the  $K_e$  of spruce timber loaded parallel to the grain in a half-hole tests was found 65–75% higher compared to results from full-hole tests [13]. The smaller difference in  $K_e$  between test specimen configurations reported in that study compared the findings in this study may be explained by the lower  $t/d$ -ratio (3.3 versus 3.8) and/or the use of global instead of local displacement, but could also be caused by differences in density or MC of the wood, which were not reported in that study. Indeed, when  $u$  was used instead of  $w$  to obtain  $K$ -values, the difference in  $K_e$  between test specimen configurations was 120–130% instead of 200–280% (Table 2). An additional comparison between  $K$ -values from a full-hole embedment test with fixed supports and a low  $t/d$ -ratio (e.g. 1.5–2) and a half-hole test, is needed to conclude whether dowel bending needs to be prevented nearly 100% or whether it is more important to include the wood material around the dowel to obtain accurate values of  $K$ .

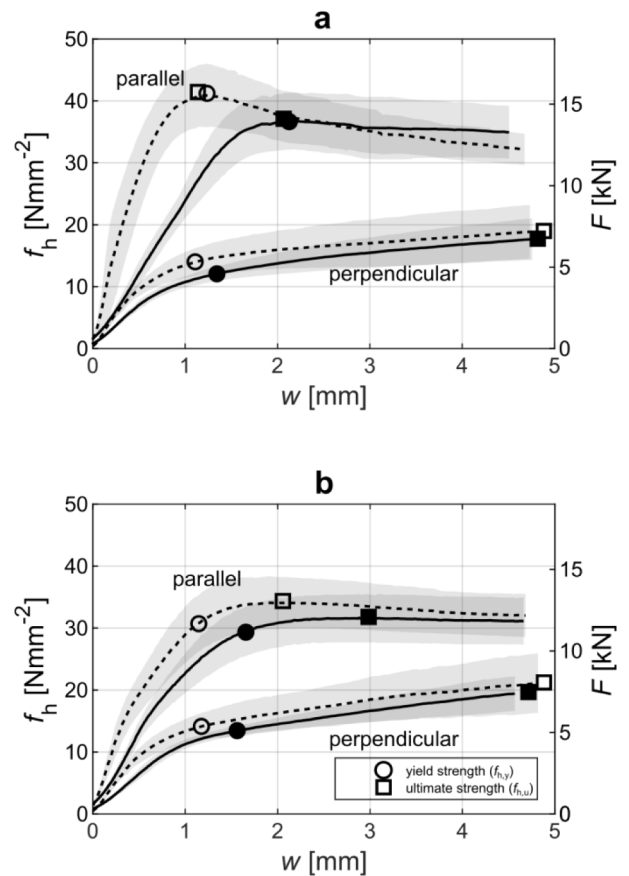


Fig. 10. Mean load–displacement curves including 95% CIs of a TM spruce and b spruce samples conditioned at 65% RH, and loaded in the full-hole (solid lines/filled markers) and half-hole (dashed lines/non-filled markers) test setup. Legend given in b.

4.8. Influence of moisture: service class 1 versus 2

The results in Table 2 show that  $f_h$  was reduced by 10–20% for TM spruce and spruce timber in service class 2 compared to 1, independent of load direction and test specimen configuration. This difference was similar between TM spruce and spruce, and shown in Fig. 11 as an example. In detail,  $f_{h,y}$  and  $f_{h,u}$  parallel to the grain were on average 19% lower for specimens with a higher MC (Table 1 and Table 2). The same comparison for loading perpendicular to the grain showed that  $f_{h,y}$  and  $f_{h,u}$  were on average 16% lower for samples with a higher MC. Strength and stiffness properties are typically inversely related to MC for MCs below the fibre saturation point, while the degree of the effect depends on the property and the MC difference [14,15]. Independent of test specimen configuration and treatment level, the percentage change in  $f_h$  parallel to the grain was around 4–7% for each percentage point difference in moisture content (1%  $\Delta$ MC) (Table 2). This is in line with previous results on the effect of MC on the compressive and embedment strength parallel to the grain that showed a 2–6% change for 1%  $\Delta$ MC for various unmodified hardwood and softwood species [14,26,17,31]. The effect of MC on  $f_h$  perpendicular to the grain of spruce was also in accordance with the literature [17], i.e. 3–4% change for 1%  $\Delta$ MC. However, for TM spruce these numbers were 6–7%, which could be related to the difference in mode of failure between spruce and TM spruce, and the difference in the degree of the effect that MC differences have on various strength properties (see Section “Failure modes”) [14].

Alike embedment strength, the initial foundation modulus of TM spruce was affected by the MC similar to that of spruce. On average,  $K_s$  was lower for TM spruce and spruce with higher MC independent of test specimen configuration—approximately 30% for the parallel and 20%

for the perpendicular to the grain load situation (Table 2 and Fig. 11). The displacement at the various load levels was in agreement with these observations and in general larger for samples with a higher MC. In contrast, high or low MC had no significant effect on the elastic foundation modulus of neither TM spruce nor spruce, and on average  $K_e$  was only 4% lower for specimens conditioned at 85% RH. This implies that MC mainly affects non-recoverable (plastic) deformations during embedment tests, such as fibre buckling (see Section “Surface strain”). The higher sensitivity of wood to fibre buckling with MC was discussed earlier [7], but a more thorough study is required to support this hypothesis.

4.9. Influence of gauge points: local versus global displacement

Fig. 12 shows an example of force–displacement data from the LVDTs (local displacement,  $w$ ) and from the crosshead of the testing machine (global displacement,  $u$ ) for two matched spruce specimens, average in density. In general, the  $F-u$  and  $F-w$  curve follow the same trend, and, as expected, the global displacements  $u$  are larger than the local displacements  $w$  for the same load level. This is because when the MTS machine measures displacement, it includes slip at onset of loading, which explains the offset between the two curves in Fig. 12a, b. Other differences between these two curves are the slopes of initial loading and of the unloading–reloading cycle (Fig. 12a, detail K). These slopes logically appear steeper or ‘stiffer’ for a more local measurement of displacement, since deformations that can occur in other parts of the test setup (i.e. in the timber specimen, the load fixture, the steel support and the crosshead) were precluded. The result is that, at similar force,  $w$  is smaller than  $u$  (Fig. 12). This effect is well known, and, for example, EN

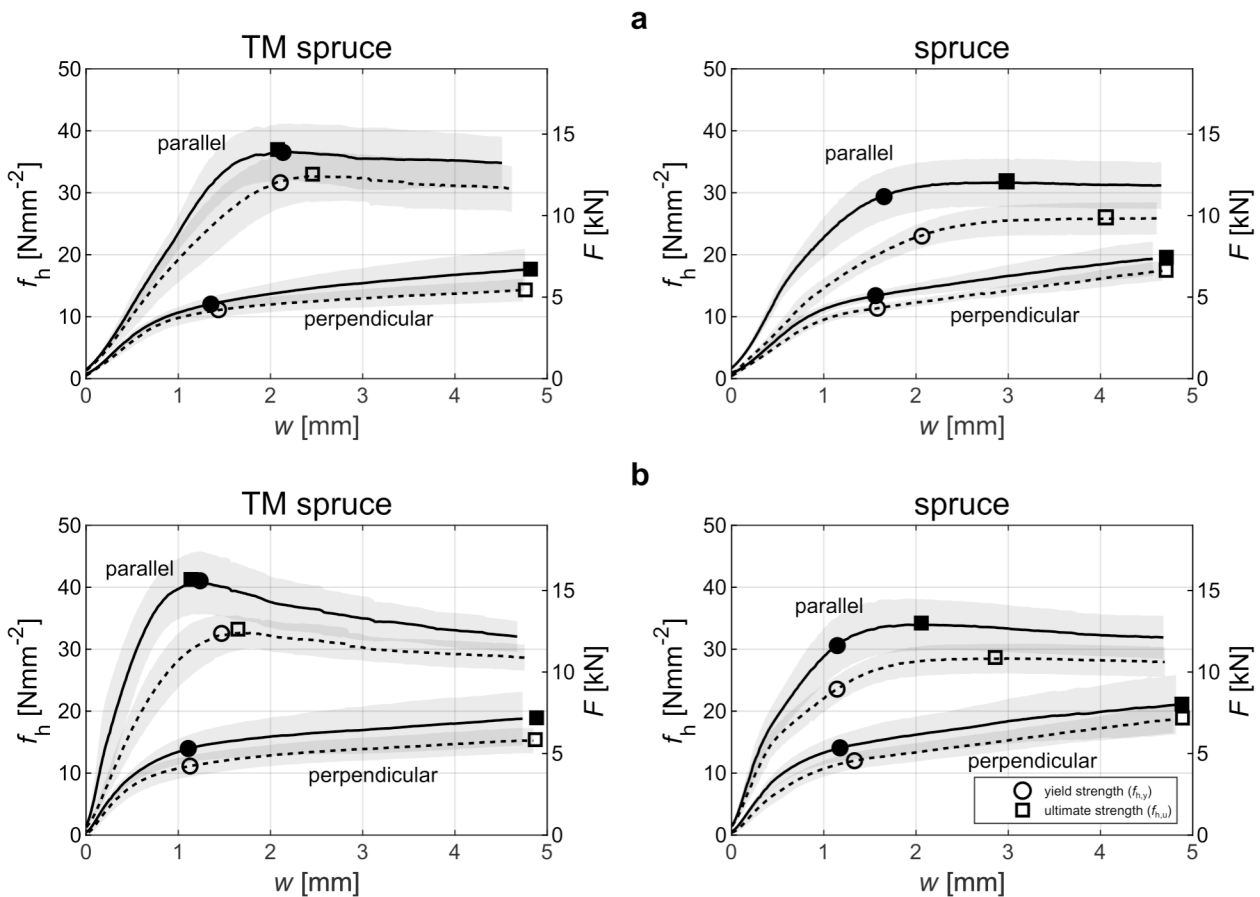


Fig. 11. Mean load–displacement curves including 95% CIs of TM spruce and spruce samples conditioned at 65% RH (solid lines) and 85% RH (dashed lines), and loaded in the a full-hole and b half-hole test setup. Legend given in b.

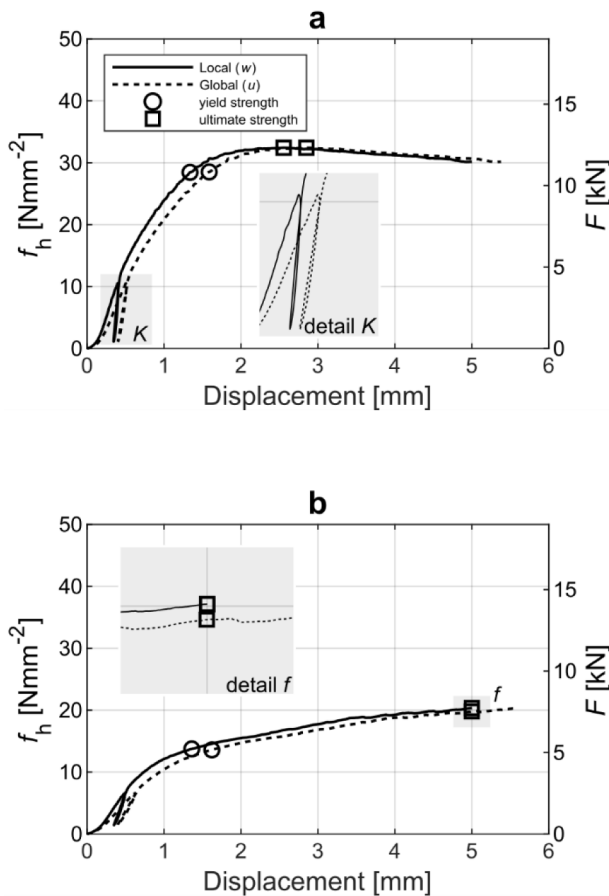


Fig. 12. Example of load–displacement data from LVDTs ( $w$ ) and crosshead ( $u$ ) for matched spruce specimens conditioned at 65% RH and loaded a parallel to grain and b perpendicular to grain in the half-hole test setup.

383 prescribes a correction method that takes account for the stiffness characteristics of the fixture, support, and test machine.

The percentage difference in mean values of embedment stiffness and strength from global versus local displacement were similar between TM spruce and spruce (Table 3). How displacement was measured, locally or globally, had a significant effect on the values of stiffness determined from embedment tests as shown in Table 3. The embedment stiffness is lower when calculated from  $u$  compared to  $w$ —10–50%, depending mainly on test specimen configuration, stiffness property (initial or elastic) and load direction. Overall, this difference was larger for  $K_e$  than for  $K_s$ , larger in half-hole than in full-hole tests, and larger for loading parallel to the grain than for loading perpendicular to the grain. How displacement was measured, practically had no influence on  $f_{h,y}$ , and differences never exceeded  $\pm 1\%$  (Table 3). How displacement was measured, only affected  $f_{h,u}$  when the ultimate strength was found at maximum displacement (Fig. 12b). This typically occurs for loading situations perpendicular to the grain (Table 2 and Table 3), but the differences were small. In detail,  $f_{h,u}$  was 1–2% lower in full-hole tests and 2–7% lower in half-hole tests when obtained from  $u$  instead of  $w$ . Since local displacement is smaller than global displacement, the values of  $f_{h,u}$  are conservative for global measurements.

#### 4.10. Influence of calculation method: yield versus ultimate strength

The difference in embedment strength perpendicular to the grain as a result of calculation method (i.e.  $f_{h,y}$  versus  $f_{h,u}$ ), as was discussed before by others (e.g. [33]), was 10% smaller for TM spruce than for spruce (Table 2). This difference mainly relates to the slope of the load–displacement curve after yielding [13]. Since this slope is less steep

after thermal modification (Fig. 8), the difference between  $f_{h,y}$  and  $f_{h,u}$  becomes smaller (on average, 38% for TM spruce versus 54% for spruce). For the load situation parallel to the grain the calculation procedure did not influence the embedment strength of TM spruce (Fig. 8), whereas for spruce differences were 10% for samples conditioned at the standard reference climate and up to 20% for the samples conditioned at 85% RH (Table 2). In contrast to the literature [33,32], perfect elastic–plastic behaviour in embedment tests parallel to the grain was not observed for spruce. In addition, the negative slope after yielding during parallel-to-grain loading has been observed earlier [13], but this slope appears much steeper for TM spruce than for spruce, i.e. after thermal modification, in particular for the half-hole test setup (Fig. 8b). This phenomenon would not have been observed if the tests ran force control. Besides stiffness and strength from bending tests, the literature on the effect of thermal modification on fundamental stress states (tension, compression and shear) and the behaviour of thermally modified timber during failure is scarce, which makes it hard to explain the change in slope after yielding (for both load situations). All specimens retained a large part of their load-carrying capacity up to the end of tests, which was true even for TM spruce specimens (Fig. 8, Fig. 10, and Fig. 11).

Table 3  
Percentage difference in mean values of embedment stiffness and strength from global ( $u$ ) versus local ( $w$ ) displacement.

Treatment	RH [%]	Stiffness			Strength	
		$K_s$	$K_e^-$	$K_e^+$	$f_{h,y}$	$f_{h,u}$
PARALLEL TO GRAIN						
Full-hole test						
Spruce	65	-17%	-25%	-23%	1%	0%
		**	**	**		
Spruce	85	-11%	-30%	-23%	0%*	0%
		**	**	**		
TM spruce	65	-15%	-26%	-22%	0%	0%
		**	**	**		
TM spruce	85	-14%	-26%	-22%	0%	0%
		**	**	**		
Half-hole test						
Spruce	65	-26%	-47%	-43%	1%	0%
		**	**	**		
Spruce	85	-21%	-43%	-39%	0%	0%
		**	**	**		
TM spruce	65	-29%*	-50%	-46%	0%	0%
		**	**	**		
TM spruce	85	-21%	-49%	-45%	1%	0%
		**	**	**		
PERPENDICULAR TO GRAIN						
Full-hole test						
Spruce	65	-10%	-15%	-14%	0%	-2%*
		**	**	**		
Spruce	85	-11%	-17%	-16%	0%	-2%
		**	**	**		**
TM spruce	65	-11%	-16%	-16%	-1%*	-2%
		**	**	**		**
TM spruce	85	-11%	-18%	-18%	-1%*	-1%
		**	**	**		**
Half-hole test						
Spruce	65	-24%	-36%	-35%	-1%	-7%
		**	**	**	**	**
Spruce	85	-25%	-38%	-36%	-1%	-5%
		**	**	**	**	**
TM spruce	65	-29%	-42%	-41%	0%	-5%
		**	**	**		**
TM spruce	85	-27%	-43%	-41%	0%*	-2%
		**	**	**		**

Statistical test: dependent t-tests for differences in mean values. Significance levels: \*\*  $p < 0.01$ , \*  $p < 0.05$ .

## 5. Conclusions

The embedment strength parallel to the grain increased by  $\sim 25\%$  due to thermal modification, while a decrease of  $\sim 10\%$  was found when load was applied perpendicular to the grain. A large share of this increase was explained by the change in the physical properties, i.e. the lowered equilibrium moisture content, due to thermal modification, while this decrease is mainly a result of the degradation of wood polymers. The influence of the investigated parameters on embedment properties of unmodified timber were in line with literature. After thermal modification, the results followed similar trends as before. That is, (1) embedment strength and density were correlated; (2) load direction considerably affected both embedment strength and stiffness; (3) test specimen configuration, full hole versus half hole, had no clear influence on embedment strength, but clearly affected values of embedment stiffness, independent of the direction of loading; (4) both embedment strength and initial foundation modulus were lower for specimens with a higher moisture content, but no such difference was found for the elastic foundation modulus; (5) measuring displacement locally instead of globally had little influence on embedment strength, but largely affected embedment stiffness, and; (6) embedment strength perpendicular to the grain different considerably between calculation methods (yield versus ultimate strength). Independent of treatment level, the embedment strength was most influenced by load direction (30–70% difference), followed by calculation method (30–60% difference, but only for perpendicular to grain) and the level of moisture content (10–20% difference). While the embedment stiffness was most influenced by the test specimen configuration (40–280% difference), followed by the gauge points for displacement measurement (10–50% difference) and moisture content (10–50% difference, but only for the initial foundation modulus). However in contrast to unmodified timber, the influence of load direction on embedment strength was  $\sim 30\%$  larger and the influence of calculation method on embedment strength perpendicular to the grain was  $\sim 10\%$  smaller after thermal modification.

## 6. Future studies

Although thermally modified spruce timber is more sensitive to splitting failure than unmodified spruce timber, the tests performed in this study highlight possibilities for a ductile design in thermally modified timber (TMT), where ductility could be provided by reinforced connections. Yet, from a practical and economical point of view, it can be argued if it is feasible to reinforce connections in TMT. In addition, to assess the necessity of reinforced connections in TMT, embedment properties should be evaluated without reinforcement as well. Important topics for future research regarding connections in TMT are: (1) relationships between embedment strength and predictors (e.g. density), (2) assessment of the sensitivity to splitting failure in joints with dowel-type fasteners loaded in shear, (3) design solutions to introduce a ductile behaviour, and (4) the influence of service class 3 conditions on embedment properties.

## CRedit authorship contribution statement

**Joran Blokland:** Conceptualization, Methodology, Validation, Formal analysis, Investigation, Data curation, Writing - original draft, Writing - review & editing, Visualization, Project administration. **Sara Florisson:** Conceptualization, Methodology, Validation, Investigation, Data curation, Writing - original draft, Writing - review & editing, Project administration. **Michael Schweigler:** Conceptualization, Methodology, Writing - review & editing. **Torbjörn Ekevid:** Conceptualization, Methodology, Supervision, Funding acquisition. **Thomas K. Bader:** Resources, Writing - review & editing, Funding acquisition. **Stergios Adamopoulos:** Resources, Writing - review & editing, Funding acquisition.

## Declaration of Competing Interest

The authors declare that they have no known competing financial interests or personal relationships that could have appeared to influence the work reported in this paper.

## Acknowledgements

The laboratory apparatuses were provided by the Department of Building Technology, Linnaeus University, Växjö, Sweden. The timber and thermal modification were provided by Stora Enso Timber AB, Sweden.

## Data availability

The data is available upon reasonable request.

## References

- [1] M. Arnold, Effect of moisture on the bending properties of thermally modified beech and spruce, *J. Mater. Sci.* 45 (3) (2010) 669–680.
- [2] ASTM D 5764-97a, Standard test method for evaluating dowel-bearing strength of wood and wood-based products. American Society for Testing and Materials (ASTM), West Conshohocken, PA, 2013.
- [3] T.K. Bader, K. Hofstetter, G. Alfredsen, S. Bollmus, Changes in microstructure and stiffness of Scots pine (*Pinus sylvestris* L) sapwood degraded by *Gloeophyllum trabeum* and *Trametes versicolor* – Part II: Anisotropic stiffness properties, *Holzforsch* 66 (2011) 199–206.
- [4] M.J. Boonstra, J. Van Acker, B.F. Tjeerdma, E.V. Kegel, Strength properties of thermally modified softwoods and its relation to polymeric structural wood constituents, Propriétés mécaniques de bois résineux modifiés par traitement thermique en relation avec la constitution en polymères ligneux structuraux, *Ann. For. Sci.* 64 (7) (2007) 679–690.
- [5] C. Cai, H. Heräjärvi, A. Haapala, Effects of environmental conditions on physical and mechanical properties of thermally modified wood, *Can. J. For. Res.* 49 (11) (2019) 1434–1440.
- [6] H. Cruz, S. Rodrigues, A. Gomes, Embedding and withdrawal resistance of screws on thermal treated wood. In: Proc. of the 7<sup>th</sup> European Conference on Wood Modification (ECWM), Lisbon, Portugal, 2014.
- [7] J.M. Dinwoodie, *Timber: its nature and behaviour*, Taylor & Francis Abingdon, Oxon, UK, 2000.
- [8] J. Ehlbeck, H. Werner, Softwood and hardwood embedding strength for dowel-type fasteners. In: CIB-W18 Paper 25-7-2, Åhus, Sweden, 1992.
- [9] EN 383, Timber Structures—Test methods—Determination of embedment strength and foundation values for dowel type fasteners. European Committee for Standardization (CEN), Brussels, 2007.
- [10] EN 1993-1-8, Design of steel structures—Part 1-8: Design of joints. European Committee for Standardization (CEN), Brussels, 2005.
- [11] EN 1995-1-1, Design of timber structures—Part 1-1: General—Common rules and rules for buildings. European Committee for Standardization (CEN), Brussels, 2011.
- [12] G. Fajdiga, B. Zafošnik, B. Gospodarič, A. Straže, Compression tests of thermally-treated beach wood: experimental and numerical analysis, *BioResources* 11 (1) (2016) 223–234.
- [13] S. Franke, N. Magnière, Discussion of testing and evaluation methods for the embedment behaviour of connections, in: Proc. of the International Network on Timber Engineering Research (INTER), Bath, UK, 2014.
- [14] C.C. Gerhards, Effect of moisture content and temperature on the mechanical properties of wood: An analysis of immediate effects, *Wood Fiber* 14 (1) (1982) 4–36.
- [15] D.W. Green, J.E. Winandy, D.E. Kretschmann, Mechanical properties of wood, in: *Wood handbook—Wood as an engineering material*, U.S. Department of Agriculture, Forest Service, Forest Products Laboratory, Madison, WI, 1999, pp 1–45.
- [16] J. Hamada, A. Pétrissans, F. Mothe, J. Ruelle, M. Pétrissans, P. Gérardin, Variation in the natural density of European oak wood affect thermal degradation during thermal modification, *Ann. For. Sci.* 73 (2016) 277–286.
- [17] U. Hübner, T. Bogensperger, G. Schickhofer, Embedding strength of European hardwoods. In: CIB-W18 Meeting 41 Paper 41-7-5, Växjö, Sweden, 2008.
- [18] International ThermoWood Association, *ThermoWood Handbook*, Helsinki, Finland, 2003.
- [19] J. Jermer, C. Bengtsson, F. Brem, A. Clang, B. Ek-Olausson, M.-L. Edlund, Heat-treated wood—Durability and technical properties. Tech. Rep. 25, SP Swedish National Testing and Research Institute, 2003.
- [20] Y. Kubojima, T. Okano, M. Ohta, Bending strength and toughness of heat-treated wood, *J. Wood Sci.* 46 (1) (2000) 8–15.
- [21] W. Lederer, T.K. Bader, L. Muszynski, J. Eberhardsteiner, Exploring a multi-modal experimental approach to investigation of local embedment behaviour of wood under steel dowels, *Strain* 52 (6) (2016) 531–547.

- [22] W. Lederer, T.K. Bader, G. Unger, J. Eberhardsteiner, Influence of different types of reinforcements on the embedment behaviour of steel dowels in wood, *Eur. J. Wood Prod.* 74 (6) (2016) 793–807.
- [23] A. Leijten, J. Köhler, A. Jorissen, Review of probability data for timber connections with dowel-type fasteners. In: CIB-W18 Paper 37-7-13, Edinburgh, UK, 2004.
- [24] H. Militz, M. Altgen, Processes and properties of thermally modified wood manufactured in Europe, in: Deterioration and protection of sustainable biomaterials (vol 982, pp 269-285), ACS Symposium Series, 2014.
- [25] H. Pleschberger, A. Teischinger, U. Müller, C. Hansmann, Change in fracturing and colouring of solid spruce and ash wood after thermal modification, *Wood Mat. Sci. Eng.* 9 (2) (2014) 92–101.
- [26] D.R. Rammer, S.G. Winistorfer, Effect of moisture content on dowel-bearing strength, *Wood Fiber Sci.* 33 (1) (2001) 126–139.
- [27] A. Reiterer, G. Sinn, Fracture behaviour of modified spruce wood: a study using linear and non linear fracture mechanics, *Holzforsch* 56 (2002) 191–198.
- [28] E. Roszyk, E. Stachowska, J. Majka, P. Mania, M. Broda, Moisture-dependent strength properties of thermally-modified *Fraxinus excelsior* wood in compression, *Materials* 13 (7) (2020) 1647.
- [29] R.M. Rowell, I. Andersone, B. Andersons, Heat Treatment. In: Rowell RM (ed), *Handbook of wood chemistry and wood composites*, CRC Press LLC, Boca Raton, FL, 2013, pp. 511–536.
- [30] R.M. Rowell, R.E. Ibach, J. McSweeney, T. Nilsson, Understanding decay resistance, dimensional stability and strength changes in heat treated and acetylated wood. In: Proc. of the 4<sup>th</sup> European Conference on Wood Modification (ECWM), Stockholm, Sweden, 2009, pp 489–502.
- [31] C. Sandhaas, G.J.P. Ravenshorst, H.J. Blass, J.W.G. van de Kuilen, Embedment test parallel-to-grain and ductility aspects using various wood species, *Eur. J. Wood Prod.* 71 (2013) 599–608.
- [32] C.L. Santos, A.M.P. de Jesus, J.J.L. Morais, J.L.P.C. Lousada, A comparison between the EN 383 and ASTM D5764 test methods for dowel-bearing strength assessment of wood: experimental and numerical investigations, *Strain* 46 (2010) 159–174.
- [33] K. Sawata, M. Yasumura, Determination of embedding strength of wood for dowel-type fasteners, *J. Wood Sci.* 48 (2) (2002) 138–146.
- [34] M. Schweigler, T.K. Bader, G. Hochreiner, G. Unger, J. Eberhardsteiner, Load-to-grain angle dependence of the embedment behavior of dowel-type fasteners in laminated veneer lumber, *Constr. Build. Mater.* 126 (2016) 1020–1033.
- [35] A.J. Stamm, K. Horace, K. Burr, A.A. Kline, Staywood—Heat-stabilized wood, *Ind. Eng. Chem.* 38 (6) (1946) 630–634.
- [36] J. van Blokland, Thermally modified timber: Novel aspects of bending behaviour towards grading and structural applications, Linnaeus University Dissertations, Växjö, 2020.
- [37] J. van Blokland, A. Olsson, J. Oscarsson, S. Adamopoulos, Prediction of bending strength of thermally modified timber using high-resolution scanning of fibre direction, *Eur. J. Wood Prod.* 77 (3) (2019) 327–340.
- [38] L.R.J. Whale, I. Smith, A method for measuring the embedding characteristics of wood and wood-based materials, *Mater. Struct.* 22 (6) (1989) 403–410.
- [39] R. Widmann, J.L. Fernandez-Cabo, R. Steiger, Mechanical properties of thermally modified beech timber for structural purposes, *Mechanische Eigenschaften von thermisch modifiziertem Buchenholz für tragende Bauteile*, *Eur. J. Wood Prod.* 70 (6) (2012) 775–784.
- [40] E. Windeisen, H. Bächle, B. Zimmer, G. Wegener, Relations between chemical changes and mechanical properties of thermally treated wood, *Holzforsch* 63 (2009) 773–778.